Australian Journal of Earth Sciences
Publication details, including instructions for authors and subscription information:
http://www.informaworld.com/smpp/title~content=t716100753

Structure of the Tasmanian lithosphere from 3D seismic tomography

N. Rawlinson[a]; H. Tkalčić[a]; A. M. Reading[b]
[a] Research School of Earth Sciences, Australian National University, ACT, Australia [b] School of Earth Sciences and ARC Centre of Excellence in Ore Deposits, University of Tasmania, Hobart, Tas, Australia

Online publication date: 18 May 2010

To cite this Article Rawlinson, N. , Tkalčić, H. and Reading, A. M.(2010) 'Structure of the Tasmanian lithosphere from 3D seismic tomography', Australian Journal of Earth Sciences, 57: 4, 381 — 394
To link to this Article: DOI: 10.1080/08120099.2010.481325
URL: http://dx.doi.org/10.1080/08120099.2010.481325

Australian Journal of Earth Sciences (2010) **57**, (381–394)

Structure of the Tasmanian lithosphere from 3D seismic tomography

N. RAWLINSON[1]*, H. TKALČIĆ[1] AND A. M. READING[2]

[1]*Research School of Earth Sciences, Australian National University, ACT 0200, Australia.*
[2]*School of Earth Sciences and ARC Centre of Excellence in Ore Deposits, University of Tasmania, Hobart, Tas 7001, Australia.*

Seismic data from three separate experiments, a marine active source survey with land-based stations, and two teleseismic arrays deployed to record distant earthquakes, are combined in a joint inversion for the 3D seismic structure of the Tasmanian lithosphere. In total, travel-time information from nearly 14 000 source–receiver paths are used to constrain a detailed model of crustal velocity, Moho geometry and upper mantle velocity beneath the entire island. Synthetic reconstruction tests show good resolution beneath most of Tasmania with the exception of the southwest, where data coverage is sparse. The final model exhibits a number of well-constrained features that have important ramifications for the interpretation of Tasmanian tectonic history. The most prominent of these is a marked easterly transition from lower velocity crust to higher velocity crust which extends from the north coast, northeast of the Tamar River, down to the east coast. Other significant anomalies include elevated crustal velocities beneath the Mt Read Volcanics and Forth Metamorphic Complex; thickened crust beneath the Port Sorell and Badger Head Blocks in central northern Tasmania; and distinctly thinner, higher velocity crust beneath the Rocky Cape Block in northwest Tasmania. Combined with existing evidence from field mapping, potential-field surveys and geochemical data, the new results support the contention that east and west Tasmania were once passively joined as far back as the Ordovician, with the transition from lithosphere of Proterozoic continental origin to Phanerozoic oceanic origin occurring some 50 km east of the Tamar River; that the southeast margin of the Rocky Cape Block may have been a former site of subduction in the Cambrian; and that the Badger Head and Port Sorell Blocks were considerably shortened and thickened during the Cambrian Tyennan and Middle Devonian Tabberabberan Orogenies.

KEY WORDS: lithospheric structure, seismic tomography, Tasmania, Tyennan Orogen.

INTRODUCTION

Seismic tomography is a data-inference technique which requires the solution of a large inverse problem to build heterogeneous models of the Earth's interior that are consistent with observations made from seismic records. From its origins in the mid-late 1970s (Aki & Lee 1976; Aki *et al*. 1977; Dziewonski *et al*. 1977), it has developed into a mature technique that is widely used to image subsurface structure at a variety of scales. The use of many sources and receivers with an even geographical distribution is essential for producing a detailed and well-resolved seismic model. Artificial sources, such as explosions, airguns or vibroseis are often used in cross-hole, reflection or wide-angle tomography, which is favoured in exploration and continental profiling (Bishop *et al.* 1985; McMechan 1987; Williamson 1990; Zelt & White 1995; Bleibinhaus & Gebrande 2006). Earthquake sources are more common in larger-scale studies which may examine regions of the crust, lithosphere or even the whole Earth (Walck 1988; Benz *et al*. 1992; Grand *et al*. 1997; Steck *et al.* 1998; Simons *et al*. 1999; Burdick *et al*. 2008; Priestley *et al*. 2008).

In Australia, 3D seismic tomography experiments began with the continent-wide SKIPPY project (1993–1998), which involved progressive coverage of Australia using a portable array of broadband seismometers to record regional earthquakes (Zielhuis & van der Hilst 1996). Both surface wave and body wave data from SKIPPY and subsequent deployments have been used to generate 3D tomographic images of compressional and shear wave-speed variations in the upper mantle beneath Australia at a horizontal resolution of between 200 and 250 km (Zielhuis & van der Hilst 1996; Debayle & Kennett 2000; Gorbatov & Kennett 2003; Fishwick *et al.* 2005). Major results from these studies include the delineation of Archean and Proterozoic Cratons at depth, a pronounced transition from high wave speeds beneath Precambrian western and central Australia to low wave speeds beneath Phanerozoic eastern Australia, and even lower wave speeds beneath the eastern

*Corresponding author: nick@rses.anu.edu.au

ISSN 0812-0099 print/ISSN 1440-0952 online
DOI: 10.1080/08120099.2010.481325

seaboard, the latter correlating well with evidence of recent volcanism (Sutherland 2003).

Over the last decade, the emphasis in passive seismic imaging has shifted to much higher density arrays designed to target areas of particular geological interest. The first of these projects, called MALT, involved the rolling deployment of three temporary arrays of 40 short-period seismometers in western Victoria through to eastern South Australia (Graeber *et al.* 2002; Clifford *et al.* 2008). This was followed by 72 short-period and broadband seismometers deployed in Tasmania during 2002 (Rawlinson *et al.* 2006a) as part of the TIGGER experiment, and the 20 short-period seismometer SEAL array deployed in southern New South Wales and northern Victoria in 2004 (Rawlinson *et al.* 2006b). As of February 2010, there have been 12 separate temporary deployments in southeast Australia with a cumulative total of over 500 sites covering much of Tasmania, Victoria, New South Wales and southern South Australia at a station spacing of 50 km or less. The primary goal of the deployments was to record distant earthquake data for use in the teleseismic tomography that we present. Complementary techniques include ambient-noise tomography and receiver-function analysis.

In Tasmania, there have been two passive array deployments: TIGGER in 2002, which covered much of northern Tasmania, and the 40 station SETA array, which extended across the southeastern part of the state. To date, two studies have been carried out using the TIGGER data. In the first (Rawlinson *et al.* 2006a), teleseismic arrival time residuals were inverted for 3D wave-speed perturbations in the lower crust and lithospheric mantle beneath northern Tasmania. This was followed by a joint inversion of active source and teleseismic data for the crust and upper mantle structure beneath northern Tasmania (Rawlinson & Urvoy 2006). The active source data comes from the wide-angle component of the TASGO experiment (Rawlinson *et al.* 2001), which involved the deployment of 44 digital and analogue recorders throughout Tasmania to record refraction and reflection phases from the ~36 000 airgun shots produced by the RV *Rig Seismic* during its circumnavigation of Tasmania in 1995.

The aim of the current study is to simultaneously invert all teleseismic arrival time data from TIGGER and SETA, and all Pg (path refracts back to the surface above the Moho), Pn (path refracts back to the surface below the Moho) and PmP (path reflects from the Moho) travel times from the TASGO dataset to retrieve the 3D seismic structure of the Tasmanian lithosphere. This work adds significantly to the inversion results of Rawlinson & Urvoy (2006). In particular, much of the structure beneath the southern half of Tasmania is now resolved, thanks to the new constraints provided by the SETA dataset, and additional wide-angle information utilised from TASGO. The new images of lithospheric velocity and Moho geometry help shed light on several important questions regarding the provenance and evolution of the various crustal blocks that comprise Tasmania, in particular, the differences between the West and East Tasmania Terranes, and the role of the Rocky Cape Block in the Tyennan Orogeny.

TECTONIC SETTING

The Tasman Orogen, or Tasmanides (Foster & Gray 2000; Glen 2005), comprises the eastern one-third of the present-day Australian continent. The dominant period of formation took place between the Middle Cambrian and Triassic, with convergence along the proto-Pacific margin of east Gondwana (Direen & Crawford 2003a, b; Crawford *et al.* 2003a, b) producing an outward-stepping series of fold belts in the Delamerian, Lachlan, New England and Thomson Orogens. The evolution of the Lachlan Orogen, which underlies much of Victoria, may have involved multiple coeval subduction zones (Foster & Gray 2000; Fergusson 2003) or orogen-parallel strike-slip tectonics (Glen 2005), but a consensus on this issue remains elusive, with a variety of possible substrates still under consideration, from purely oceanic to mixed oceanic and continental (Glen 2005). Correspondingly, tectonic models of the region vary between a predominantly accretionary oceanic system (Foster & Gray 2000; Collins 2002; Fergusson 2003; Spaggiari *et al.* 2004) and a largely intracratonic setting (VandenBerg 1999; Willman *et al.* 2002). It has also been suggested that fragments (or 'continental ribbons') rifted from Precambrian Australia during the breakup of the supercontinent Rodinia underlie parts of the Lachlan Orogen (Direen & Crawford 2003a; Crawford *et al.* 2003a, b; Glen 2005).

Over the past few decades, there have been a number of studies that have argued (often inconsistently with one other) for the manifestation of the Lachlan Orogen in Tasmania. For example, Talent & Banks (1967) found close sedimentological and faunal similarities between the Lower Devonian Walhalla Group of eastern Victoria and fossiliferous units in quartz arenites from a quarry at Scamander (northeast Tasmania). Powell & Baillie (1992) found many stratigraphic and sedimentological similarities between the East Tasmania Terrane and the Melbourne Zone, although noted that there are differences in structural detail, particularly in the vergence of Middle Devonian folds. Leaman *et al.* (1994) used evidence from geological mapping and potential-field data to postulate that Precambrian rocks from western Tasmania comprise a series of thrust slices embedded in the western part of the Lachlan Orogen and eastern part of the Kanmantoo Fold Belt. More recently, Reed (2001) argued that outcrop in eastern Tasmania more closely resembles rocks in the Tabberabbera Zone, with the possibility that rocks exposed throughout western Tasmania may form basement to the Melbourne Zone. This latter argument is adopted by Cayley *et al.* (2002), who proposed that the Precambrian core of western Tasmania extends northward beneath Bass Strait and underlies the Melbourne Zone. One of the main difficulties in linking mainland Australia and Tasmania is that the West Tasmania Terrane (Figure 1) contains numerous outcrops of Proterozoic rocks, whereas the Lachlan Orogen contains little evidence of Precambrian exposure in the geological record (Elliot & Gray 1992). As a consequence, the position of Tasmania in plate-tectonic reconstructions, particularly in the Late Proterozoic and Early Paleozoic, remains controversial. Meffre

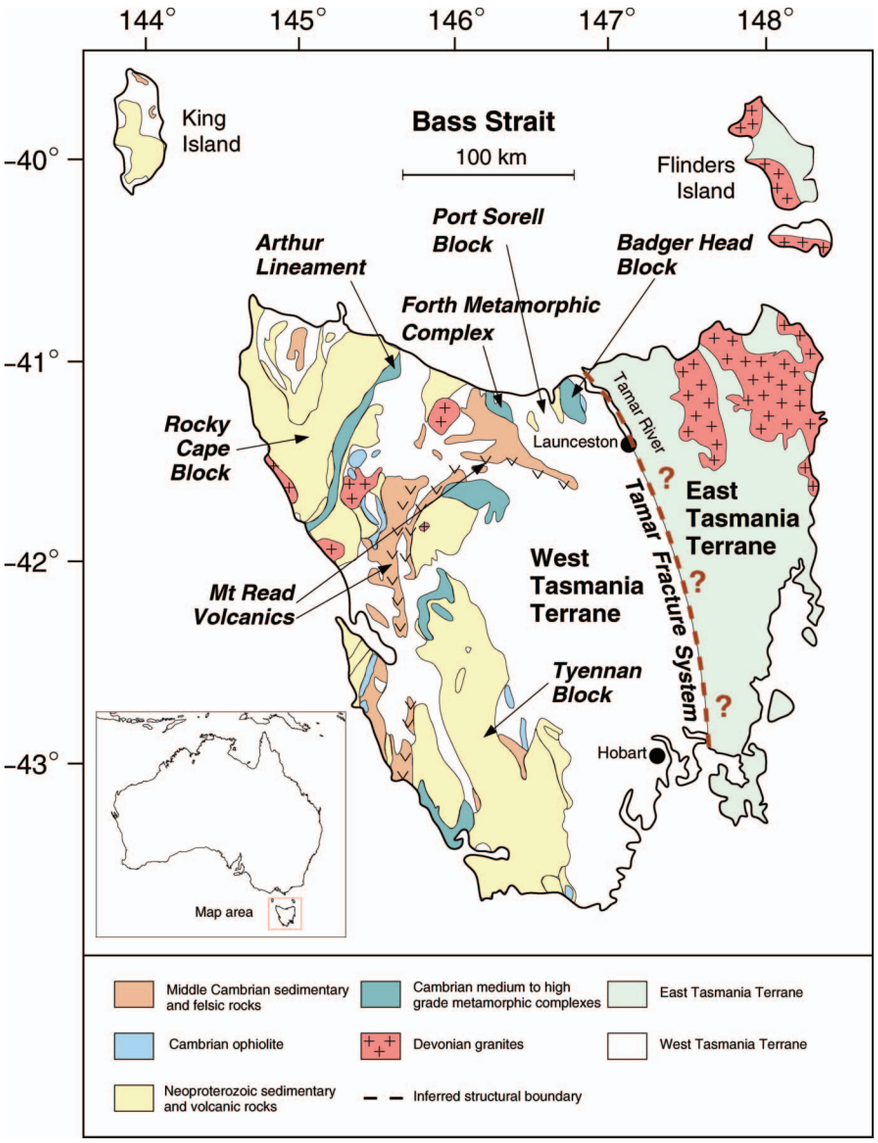

Figure 1 Simplified geological map of Tasmania showing major structural and stratotectonic features (based on Spaggiari *et al.* 2003). The boundary between the East and West Terranes is largely obscured by post-Devonian cover sequences (not shown), and is not necessarily coincident with the proposed Tamar Fracture System, the location of which is included for reference. Inset: location of map area within a regional context.

et al. (2000), discussed two possible models: one requires Tasmania to move westward to its current position, while the other requires it to move eastward. In the former case, Elliot & Gray (1992) argued that both the East and West Tasmania Terranes do not correlate with mainland Australia or northeast Victoria Land, Antarctica, and suggested that Tasmania was positioned east of mainland Australia, with possible Precambrian links to North America.

The other model (Burrett & Findlay 1984) sees a direct link between mainland Australia, Antarctica and Tasmania, with the West Tasmania Terrane attached to the Precambrian eastern margin of Gondwana between the Australian craton and Antarctica. These models tend to invoke major faulting in Bass Strait to explain the eastward migration required to move Tasmania to its present position (Veevers & Eittreim 1988). A third possibility arises from evidence that the rifted margin of East Gondwana was very irregular (in map view), with pronounced salients and re-entrants (Powell *et al.* 1990; Direen & Crawford 2003a, b); it is quite plausible for Tasmania to represent a margin salient, which would obviate the need for strike-slip faulting in Bass Strait.

The idea that Tasmania, mainland Australia and Antarctica were once part of the same Neoproterozoic margin, and therefore shared a similar tectonic evolution in the Cambrian, has gained some momentum in recent times. Direen & Crawford (2003a, b) have found paired suites of unusual ~580 Ma olivine-rich mafic volcanics, together with unusual ~515 Ma boninites in both western Tasmania and the Delamerian Orogen in Victoria, South Australia and western New South Wales, which gives credibility to the idea that the Tyennan Orogen in western Tasmania, the Delamerian Orogen and the Ross Orogen of Northern Victoria Land, Antarctica, share a common tectonic history (Li *et al.* 1997; Turner *et al.* 1998).

In a recent paper, Berry *et al.* (2008) used U–Th–Pb monazite dating to argue that the Proterozoic history of Tasmania is best correlated with the Transantarctic Mountains, and that the West Tasmania Terrane rifted from the East Antarctic margin at 580 Ma, before being

trapped outboard of the Cambrian Ross–Delamerian Orogeny. It then reconnected to Antarctica during the last stages of this deformational event. They concluded that the West Tasmania Terrane is more closely related to the Transantarctic Mountains than the Adelaide Fold Belt. As noted earlier, another perspective is supplied by Cayley *et al.* (2002), who used aeromagnetic data and field observations to suggest that the Proterozoic crust beneath western Tasmania extends across Bass Strait and underlies the younger sedimentary rocks of the Melbourne Zone in Victoria. They referred to this fragment of Proterozoic crust as the Selwyn Block, the existence of which would have dramatic implications for tectonic models that describe the assembly of the Lachlan Orogen.

At the onset of the Paleozoic Era, Tasmania largely comprised what is now referred to as the West Tasmania Terrane, which was shaped by a rift–drift–collision cycle in the Late Neoproterozoic to Late Cambrian (Crawford & Berry 1992; Crawford *et al.* 2003a). The extensional phase, possibly initiated by plume-triggered rifting (Meffre *et al.* 2004) produced rift basins, leading to volcanic passive margin formation and eventually the opening of an ocean at about 580 Ma (Direen & Crawford 2003a, b; Crawford *et al.* 2003a, b; Berry *et al.* 2008). An intraoceanic volcanic arc was then established outboard to the east of the margin at ~515 Ma which was subsequently obducted to the southwest by arc–continent collision. The collapse of thickened crust due to post-collisional extension produced the Mt Read Volcanics (Figure 1) and was followed by exhumation of the underthrust continental crust.

The East Tasmania Terrane differs significantly from the West Tasmania Terrane, in that it contains no evidence of Precambrian crust, either in outcrop or inferred from geophysical studies. More than a decade ago, the boundary between the two terranes was thought to be the result of a concealed crustal-scale shear zone called the Tamar Fracture System (Williams 1989), possibly arising from the juxtaposition of two disparate crustal elements during the Devonian Tabberabberan Orogeny. The location of the proposed boundary is included in Figure 1 as a reference location. However, there is little evidence of any significant contrast either in gravity (Leaman 1994) or high-resolution seismic tomography (Rawlinson *et al.* 2006a) corresponding with this proposed shear zone. Reed (2001) proposed an alternative model in which the East and West Tasmania Terranes were passively joined as far back as the Ordovician, with the former consisting of mafic oceanic crust, and the latter of Proterozoic siliciclastic crust. The new data and tomographic images from this study add new constraints to the deep structure beneath the East and West Tasmania Terranes, and thus contribute to an improved understanding of their relationship.

DATA AND METHOD

The data used in this study is sourced from three separate experiments: TASGO (1995), TIGGER (2002) and SETA (2006-2007). Figure 2 shows the locations of all recording stations associated with the three different experiments, plus the marine shot lines that generated the refraction and reflection data recorded by the TASGO stations. Note that due to equipment and noise problems, a subset of 21 stations from the TASGO array are utilised here (only these stations are shown in Figure 2). The TIGGER array was in place between March 2002 and August 2002, during which time it recorded 101 teleseismic events (Figure 3a) with sufficient signal to noise ratios to permit the extraction of reliable arrival time residuals (the difference between observed arrival times and those predicted by the global reference model *ak*135). The SETA array was installed in October 2006 and removed in August 2007, during which time 200 usable teleseismic events were recorded (Figure 3b). The uneven azimuthal distribution of earthquakes surrounding the TIGGER and SETA arrays means that data coverage is not uniform, with many paths impinging on the arrays from the north and east. The effect of this distribution on the resolution of the solution model will be examined in the next section.

The full teleseismic dataset used to constrain the 3D lithospheric model of Tasmania comprises 6520 arrival-time residuals from TIGGER and 5432 arrival-time residuals from SETA. For the most part, these comprise direct P phases, but the dataset also includes a number of pP, PP, PcP, ScP and PKiKP phases. In order to try and minimise the effects of uneven data coverage, all teleseismic data are stacked (on the basis of source location) into sub-bins which span 2.5° in both latitude and longitude. This has the effect of reducing the earthquake concentration in regions that exhibit frequent seismic activity (e.g. Fiji, Tonga, Indonesia). The total number of teleseismic arrival-time residuals is reduced from 11 952 to 9936 as a result of this process. The active source TASGO dataset contributes a total of 2148 PmP, 500 Pn and 1200 Pg phases, making a grand total of 13 748 P-wave travel times and arrival-time residuals for use in the joint inversion. In the case of TASGO, travel-time picks were made interactively, while the teleseismic arrival-time residuals were extracted using the semi-automated adaptive stacking method of Rawlinson & Kennett (2004). Figure 4 shows a data example from each of the three experiments. More detail regarding picking procedures and arrival-time residual extraction can be found in Rawlinson *et al.* (2001, 2006a, b).

All active- and passive-source travel-time data from the three separate experiments are combined in a simultaneous inversion for the 3D seismic structure of the Tasmanian lithosphere. A sophisticated iterative non-linear tomography code called FMTOMO (available from http://rses.anu.edu.au/~nick/fmtomo.html) is used to perform the inversion for crust and lithospheric mantle velocity structure and Moho geometry. FMTOMO combines an efficient grid-based eikonal solver, known as the fast marching method or FMM (Sethian & Popovici 1999), to solve the forward problem of travel-time prediction, and a subspace inversion scheme (Kennett *et al.* 1988) to adjust model parameters to better satisfy observations. The FMM and subspace schemes implemented by FMTOMO are described in detail by de Kool *et al.* (2006) and Rawlinson *et al.* (2006a) respectively.

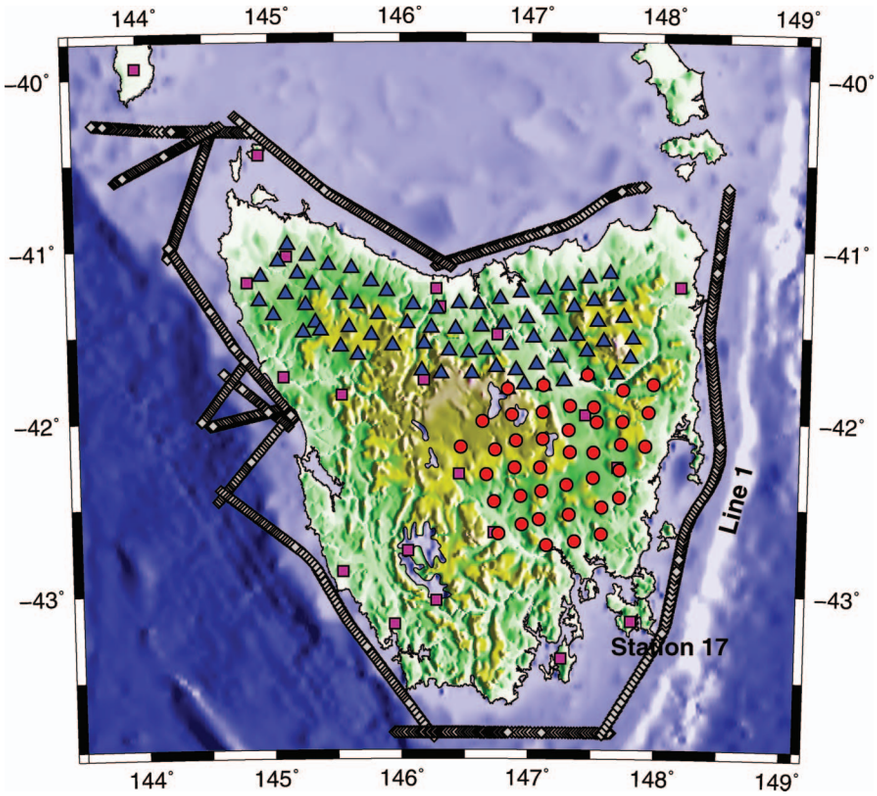

Figure 2 Location of three different seismic experiments used in this study. TIGGER stations are denoted by triangles, SETA stations by dots, and TASGO stations by squares. Contiguous grey diamonds represent the location of marine shot lines recorded by the TASGO array.

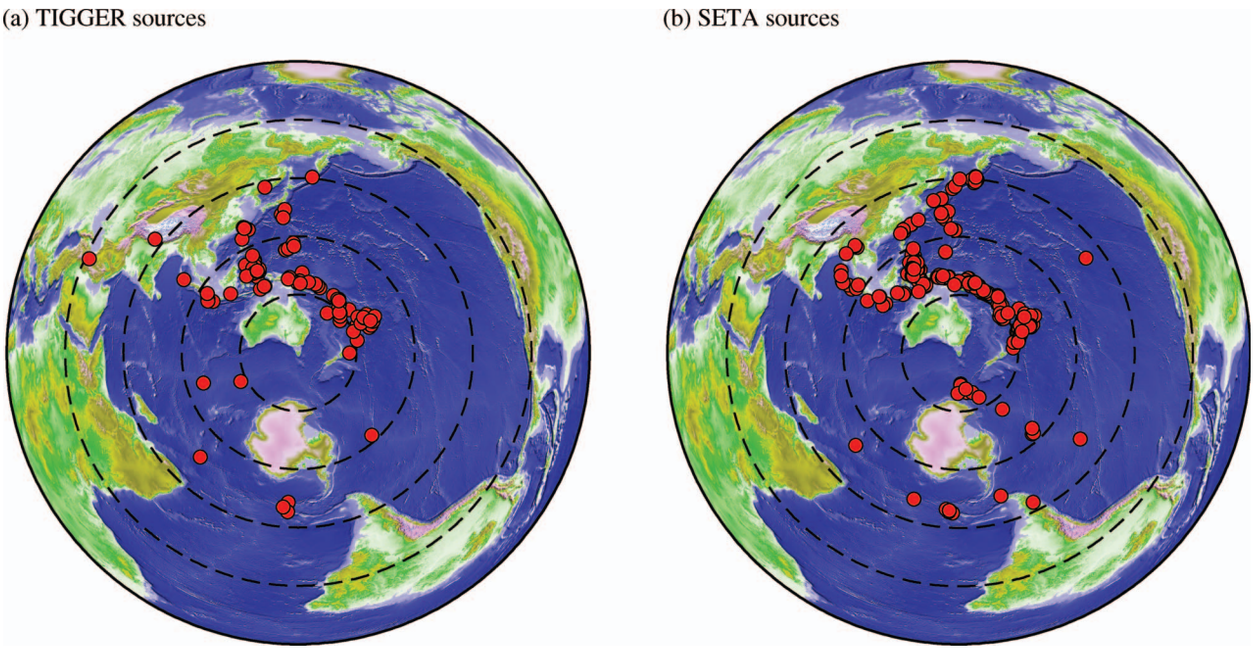

Figure 3 Location of all teleseismic sources used in this study. (a) Earthquakes detected by TIGGER array. (b) Earthquakes detected by SETA array.

RESULTS

The seismic structure of Tasmania is represented by a two-layer crust and upper mantle model in spherical coordinates. Variations in wave speed are defined by cubic B-spline volume elements that are controlled by a grid of nodes with a separation of 10 km in all three dimensions. Similarly, Moho structure is defined by cubic B-spline surface patches that are controlled by a grid of interface nodes with a spacing of 10 km. The initial or starting model in the inversion has velocity in the upper mantle defined by the global reference model

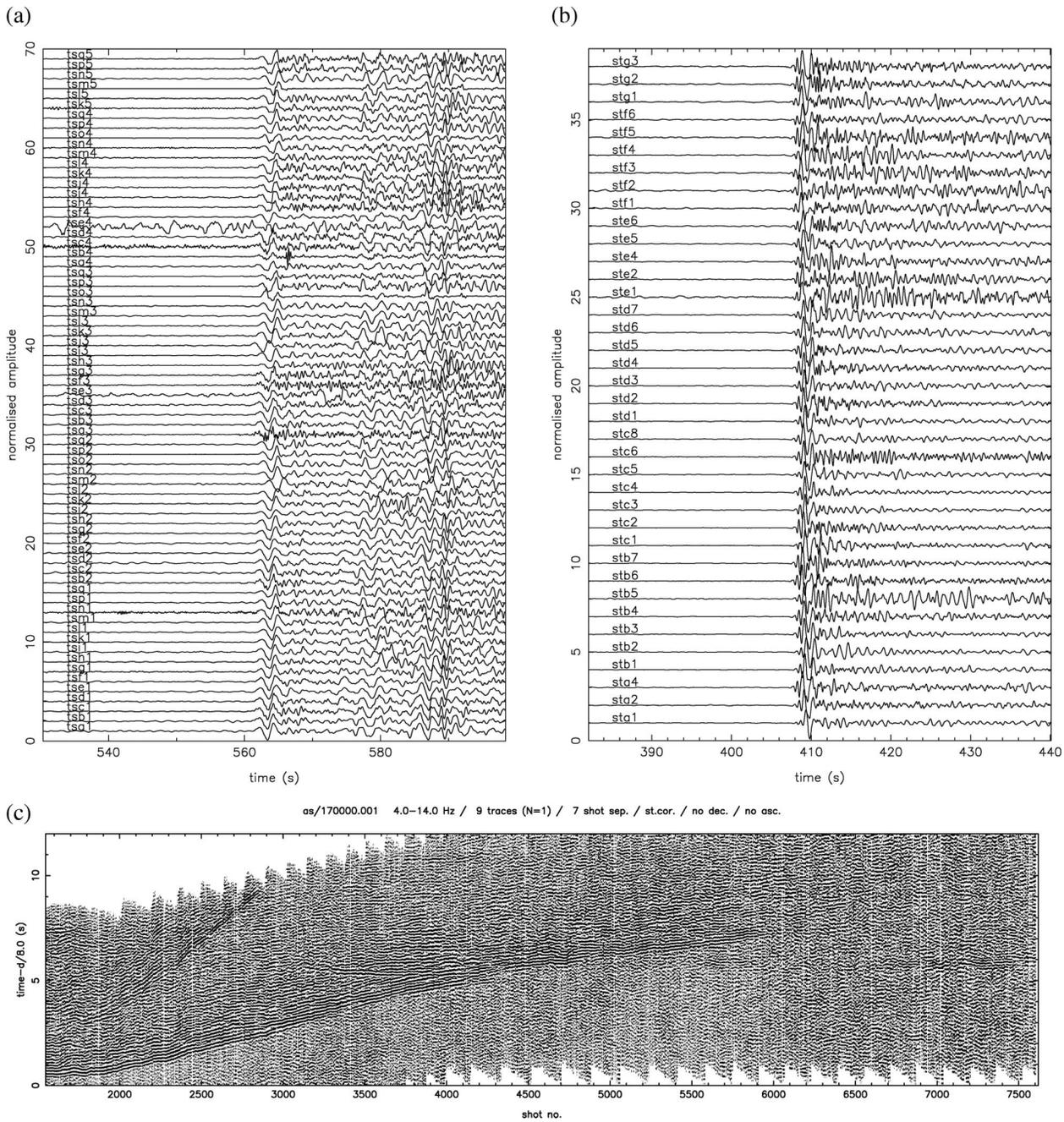

Figure 4 Examples of data recorded by each of the three arrays. (a) Magnitude 7.2 earthquake from the Mariana Islands as recorded by TIGGER. (b) Magnitude 6.1 earthquake from the New Ireland region, Papua New Guinea, as recorded by SETA. (c) Refraction profile showing shots from line 1 as recorded by station 17 of the TASGO array (see Figure 2 for location).

*ak*135 (Kennett *et al*. 1995), and crustal velocity and Moho depth defined by a locally derived 1D model of Tasmania (Rawlinson *et al*. 2001).

Synthetic resolution tests

Solution non-uniqueness—when multiple models are capable of satisfying the data—is a challenging problem to address in any seismic tomography study. It arises largely from suboptimal (insufficient and/or uneven) path coverage, together with data noise. Ideally, one would attempt to generate a large population of data-fitting models, and then interrogate them for consistent features using statistical techniques (Bodin & Sambridge 2009). However, for large inverse problems involving thousands of unknowns, this is computationally prohibitive. Another approach is to carry out so-called synthetic resolution tests (Rawlinson & Sambridge 2003), which attempt to recover a known input model from a dataset obtained by solving the forward problem using identical sources, receivers and phase types to that of the observed data. Since it is possible for

structure to be serendipitously recovered despite a lack of data constraint (e.g. a narrow thin anomaly parallel to a cluster of ray paths), and the fact that path geometry is a function of velocity heterogeneity, it is good practice to perform these tests on more than one input model.

Figure 5 shows the result of two synthetic checkerboard tests, in which the input model comprises an alternating pattern of fast and slow anomalies, and deep and shallow portions of the Moho. Gaussian noise with a standard deviation of 70 ms and 100 ms is added to the synthetic teleseismic arrival-time residuals and wide-angle travel times, respectively, in order to simulate realistic picking errors associated with the observations. The first checkerboard test (Figure 5a) aligns the positive and negative wave-speed anomalies in the crust with the deep and shallow Moho perturbations, respectively. Six iterations of FMTOMO are applied in order to recover a model that satisfies the data to the level of the imposed noise (normalised χ^2 approximately equal to 1). Due to the under-determined nature of the inverse problem, damping and smoothing are applied in order to minimise the presence of unwarranted high-amplitude anomalies and fine-scale features that are not required by the data. The quality of the recovered checkerboard pattern (Figure 5a, right) is generally good within the crust and upper mantle and along the Moho. The main exception (apart from the obvious regions outside the horizontal bounds of the source–receiver array, which are not constrained at all) is the region to the southwest, which has no teleseismic coverage and sparse active source coverage. The recovered anomalies in the crust (15 km depth slice) span a greater horizontal area than those in the upper mantle (52 km depth slice), due to the wide-angle paths being largely limited to the crust. Although in many places the pattern of anomalies is recovered accurately, the amplitude on the whole is underestimated. This can be attributed to solution non-uniqueness: models with greater amplitude will also satisfy the data, but we aim to locate the minimum structure solution, which is equally valid as far as the data are concerned. A conservative result has the advantage that it helps avoid over-interpretation of the data.

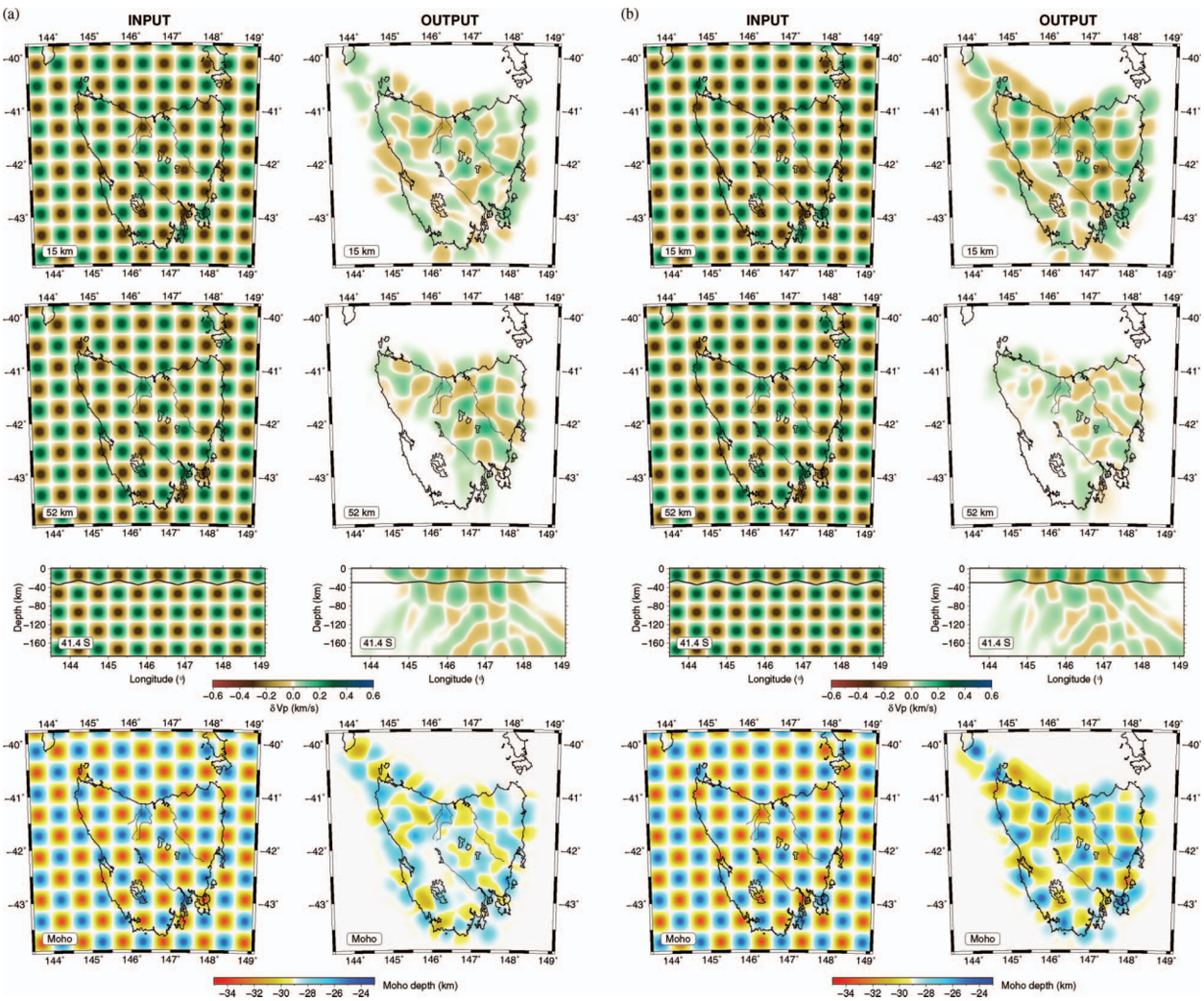

Figure 5 Synthetic checkerboard test results for the combined travel-time dataset. The difference between the tests in (a) and (b) is that the polarity of the Moho checkerboard is reversed. See text for details.

The synthetic test shown in Figure 5b is similar to that shown in Figure 5a, except that now the Moho checkerboard has reversed polarity, i.e. positive and negative wave-speed anomalies in the crust now align with shallow and deep Moho perturbations, respectively. A comparison between the recovered checkerboards in Figure 5a and b indicates that they are not of identical quality in all regions. For example, the crustal velocity perturbations (15 km depth slice) are more accurately recovered in Figure 5b compared with Figure 5a, as are the Moho anomalies. Conversely, the mantle velocity perturbations (52 km depth slice) are less accurately recovered in Figure 5b compared with Figure 5a. These differences can be attributed to the imperfect resolution of the interface depth and layer velocity trade-off. In Figure 5a, the crustal velocity and Moho perturbations do not contribute significantly to the teleseismic arrival-time residuals, as they tend to cancel each other out. Thus, there is less smearing of unresolved shallow structure back into the mantle. By contrast, in Figure 5b, the crustal velocity and Moho contributions to the teleseismic arrival-time residuals reinforce each other, and tend to dominate the signal. As a consequence, a more accurate reconstruction of crustal velocity and Moho structure is favoured by the inversion.

Despite the differences between Figure 5a and b, the synthetic tests indicate that the combined datasets resolve a significant portion of the Tasmanian lithosphere, including the structure of the Moho. A reliable interpretation of a two-layer model may be made taking account of the slight trade-off between interface structure and layer velocity. The two experiments performed here produce what can be regarded as end-member models, in that Figure 5a indicates maximum resolution of mantle velocities (and minimum resolution of crustal velocities and the Moho), while Figure 5b indicates maximum resolution of crustal velocities and Moho geometry (and minimum resolution of mantle velocities).

Lithospheric model of Tasmania

Traveltime data from TASGO, TIGGER and SETA are inverted using the same velocity and interface grid spacing, damping, smoothing and number of iterations as the synthetic checkerboard experiments of the previous section. The solution model reduces the data misfit variance by 77%, from 0.088 s^2 to 0.020 s^2, which corresponds to a reduction in the RMS residual from 296 ms to 140 ms and a reduction in the normalised χ^2 value from 11.83 to 2.83. The fact that $\chi^2 > 1$ for the solution model means that it does not fully satisfy the data, although this is commonly the case in real applications due to: (i) estimates of data uncertainty being difficult to quantify; (ii) the use of a regular and smooth parameterisation that limits the range of possible models that can be retrieved; (iii) application of explicit smoothing and damping required to stabilise the inversion; and (iv) assumptions made in the data prediction stage (in this case, that geometric ray theory is valid). Nevertheless, the final data fit is far better than that of the initial 1D model, which indicates that the recovered lateral heterogeneity is meaningful.

Figures 6 and 7 show a variety of horizontal and vertical slices through the final model, in addition to variations in Moho depth. Minimum spatial resolution in all dimensions is ~10 km (i.e. the grid spacing), although the application of implicit (due to the use of cubic splines) and explicit (via the objective function that is minimised in the inversion) smoothing means that it is generally greater. Comparison of Figure 6a and c indicates that the pattern of anomalies in the crust and upper mantle are not particularly similar, with the possible exception of northeast Tasmania (cf. Figure 7 slices CC′ and DD′). This supports the synthetic test results shown in Figure 5, which demonstrate that vertical smearing of structure between the crust and upper mantle is minimal. One of the main features of the solution model is a marked increase in crustal wave speed beneath northeast Tasmania (Figure 6a). Slices CC′ and DD′ in Figure 7 highlight this change, which also occurs in the upper mantle, although to a lesser extent. The transition to higher crustal wave speeds is matched by a reduction in Moho depth (Figure 6b) and thinning of the crust; the synthetic checkerboard tests of Figure 5 indicate that both wave speed and Moho geometry are well constrained in this region. The arcuate band of elevated wave speed in the crust along the east coast of Tasmania (Figure 6a) is not very well constrained, and may potentially trade-off with Moho depth. However, while its amplitude may be exaggerated, it still probably reflects the presence of higher velocity material (at 15 km depth) associated with a thinner crust at the continental margin.

Elevated crustal velocities can also be observed in northwest Tasmania (Figure 6a and slice BB′ in Figure 7). In the offshore region between the Tasmanian mainland and King Island, northwest–southeast smearing appears to be present, although interestingly the resolution tests indicate that the data are not completely devoid of constraint in this area. The Rocky Cape Block (Figure 1) appears to be characterised by both elevated crustal velocities and a shallow Moho, both of which are well constrained by the data.

The geometries of features in the mantle are difficult to interpret reliably, partly due to smearing in the north–south direction that is a consequence of uneven source distribution (see Figure 3); even though sub-binning has been applied in an attempt to mitigate this effect, the dominance of events from the north tends to cause structures to be smeared out along ray paths that impinge from this direction. This can be seen most clearly in slices BB′ and CC′ in Figure 7, where anomalies have a propensity to be elongated and dip to the north.

DISCUSSION AND CONCLUSIONS

The joint inversion of travel-time data from two passive-source experiments (TIGGER and SETA) and one active-source experiment (TASGO) has produced a 3D seismic model of the Tasmanian lithosphere. This new result builds on the previous work of Rawlinson *et al.* (2001, 2006a) and Rawlinson & Urvoy (2006), who utilised data from TASGO, TIGGER and, in the latter

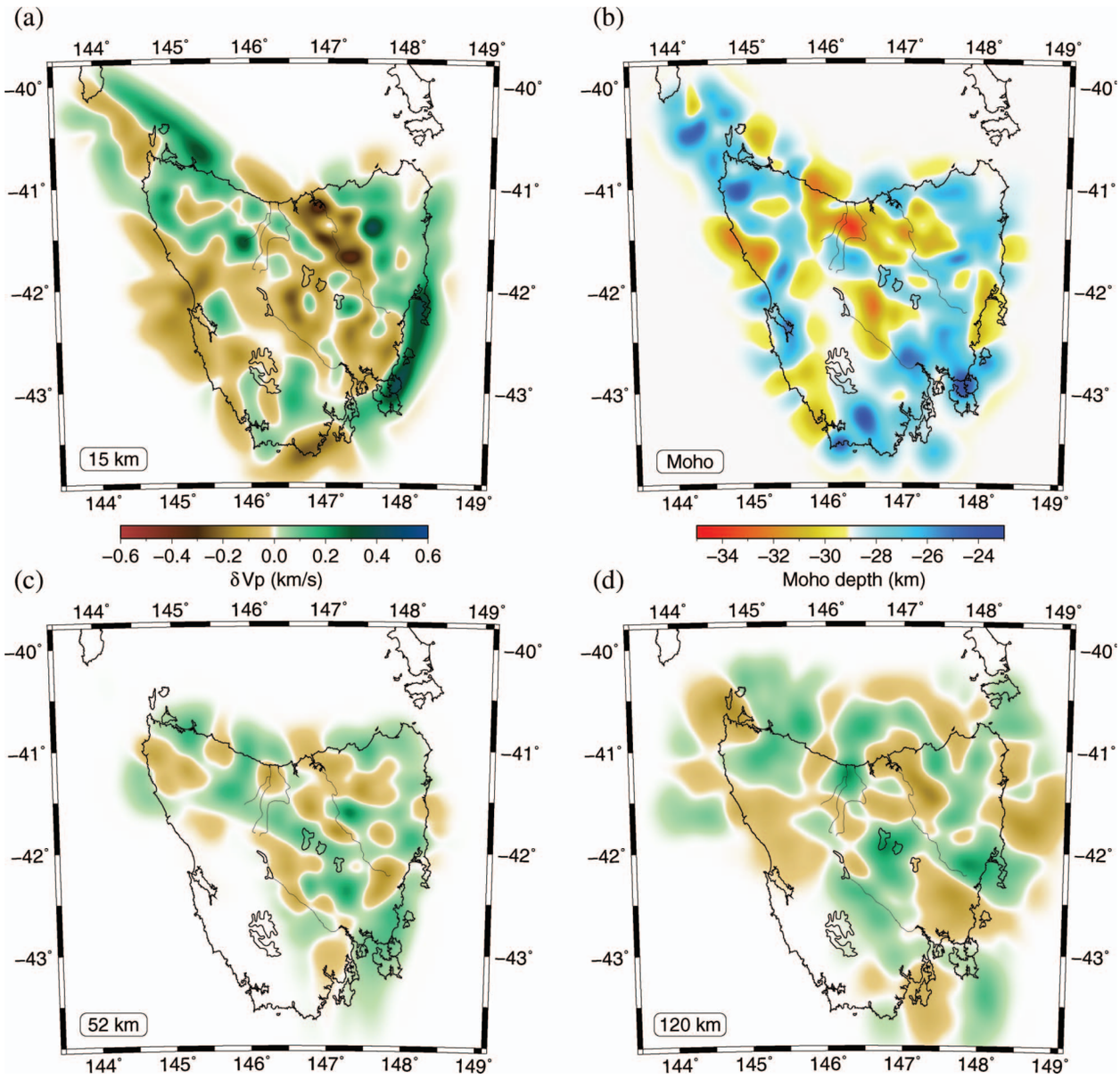

Figure 6 Horizontal slices through the 3D seismic model of the Tasmanian lithosphere at different depths (a, c, d) and variations in the recovered Moho depth (b).

case, both TASGO and TIGGER, to constrain 3D models of the Tasmanian crust and mantle lithosphere. The current study is the most complete in that it adds teleseismic arrival-time residuals from a new experiment (SETA), and exploits previously unused data from TASGO.

A number of prominent and well-constrained features are present in the seismic model of the Tasmanian lithosphere produced in this study; Figure 8 shows a selection of slices with these features highlighted. Perhaps the most significant structure of all is the dramatic transition from lower wave speeds to higher wave speeds in the crust to the northeast of the Tamar Fracture System. This variation is as much as 1.0 km/s over a horizontal distance of a few tens of kilometres. Using TASGO and TIGGER data, Rawlinson & Urvoy (2006) also observed this feature but, due to a lack of coverage, were unable to constrain its southern extent. Here, it clearly continues down to the east coast of Tasmania some 50 km east of the Tamar Fracture System. The elevated wave speeds in the crust also appear to extend into the lithospheric mantle (see slice DD′ in Figure 7), suggesting that the transition occurs throughout the full lithospheric thickness. A shallowing of the Moho, concordant with the rapid transition to elevated crustal velocities to the east of the Tamar Fracture System, can also be observed (Figure 8b), but is confined to the north and is less pronounced.

The new model presented in this paper provides strong evidence that a major change in lithospheric structure occurs to the east of the previously proposed location of the Tamar Fracture System. It is possible

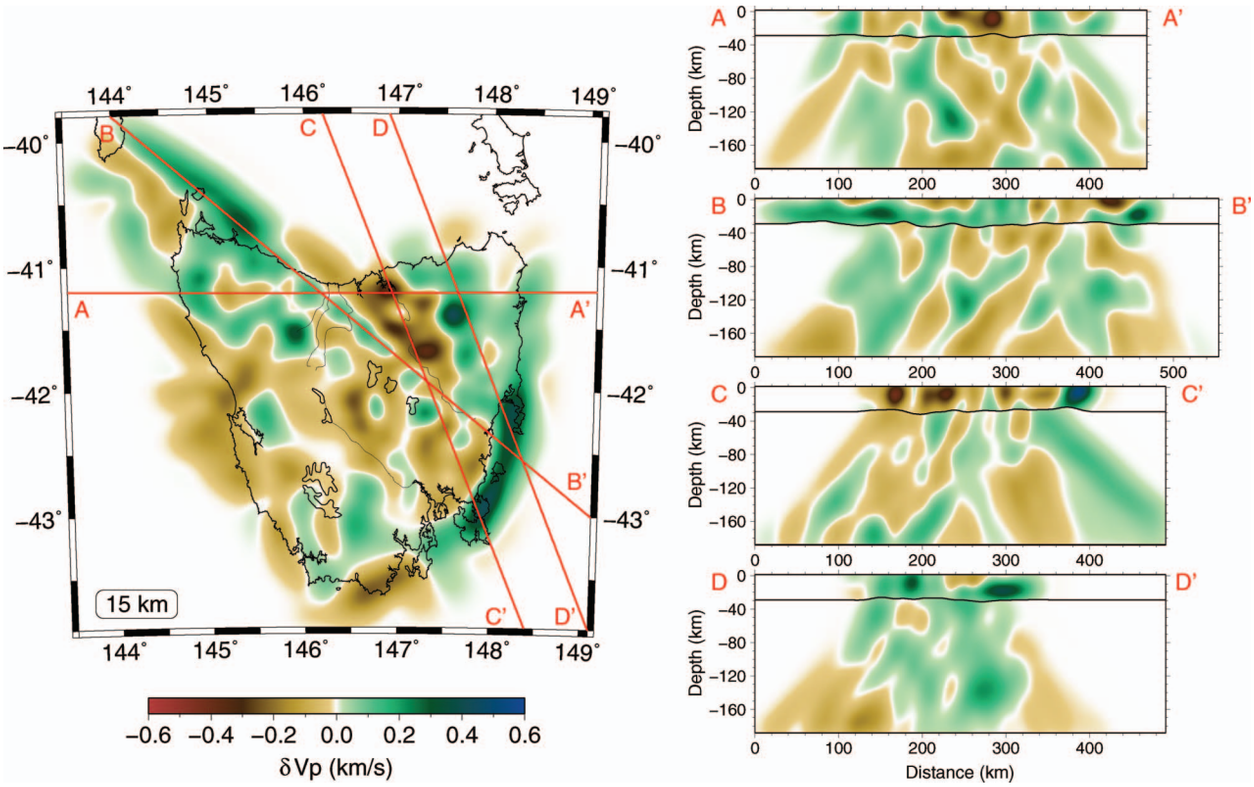

Figure 7 Great circle slices through the 3D seismic model of Tasmania. The lines superimposed on the 15 km depth slice on the left of the figure mark the locations of the vertical slices on the right.

that the Tamar Fracture System represents an upper crustal feature, mostly hidden beneath cover, which is not exactly coincident with the East to West Tasmania Terrane boundary at depth. The contrast in seismic wave speed located east of the Tamar Fracture System could be explained in terms of a juxtaposition of crustal elements during the Middle Devonian Tabberabberan Orogeny (Elliot and Gray 1992). However, it is worth considering a less dramatic alternative proposed by Reed (2001), in which the East and West Tasmania Terranes were once part of a passive margin dating back to the Ordovician, the former consisting of oceanic crust and the latter Proterozoic continental crust. Orogenic episodes from the Silurian to the Middle Devonian, interspersed with periods of sediment deposition, deformed and thickened the oceanic crust, but had little effect on the continental crust.

The idea that eastern Tasmania is underlain by mafic oceanic crust, and western Tasmania is underlain by more silicic continental crust is particularly appealing, because seismic waves typically travel faster through mafic crust compared with more felsic crust (Mooney *et al.* 1998). Thus, the elevated wave speeds observed east of the Tamar Fracture System could plausibly mark the transition from crust of Proterozoic continental origin to crust of Paleozoic oceanic origin. The relationship between the Tamar Fracture System and the paleo-continent–ocean boundary is explored by Reed (2001), who argued that differences in sedimentology and structure either side of the Tamar River are not necessarily diagnostic of an underlying major crustal shear zone. He presented an alternative hypothesis in which eastern Tasmania is thrust against western Tasmania in the Early to Middle Devonian, resulting in Paleozoic stratigraphy present on high-angle thrusts west of the Tamar River, and recumbent folding of oceanic crust east of the Tamar River. In this scenario, the Tamar Fracture System is simply an upper crustal feature related to the interaction of strongly shortened oceanic crust and a relatively small segment of detached continental crust. In Reed (2001 figure 6e), the paleo-continent–ocean boundary is placed west of the Tamar Fracture System. While this is at odds with our interpretation, in which the paleo-continent–ocean boundary is east of the Tamar Fracture System, the basic tectonic setting is in agreement.

There are a number of possible explanations as to why our results differ in detail to those of Reed (2001). For example, Reed (2001) used seismic-reflection data to constrain the location of the paleo-continent–ocean boundary, which reveal a complex zone of east-dipping reflectors. However, these structures need not be related to a change in crustal type, although they do correlate approximately with the Tiers Fault System (Direen & Leaman 1997) a major gravity and magnetic lineament in northeast Tasmania. To complicate matters further, the spatial resolution of the tomography models is not sufficient to resolve complex structures in the crust, so upper crustal features are likely to be either lost or grossly approximated, making direct comparison more difficult. Finally, the pronounced low crustal velocity region in the vicinity of the Tamar Valley corresponds

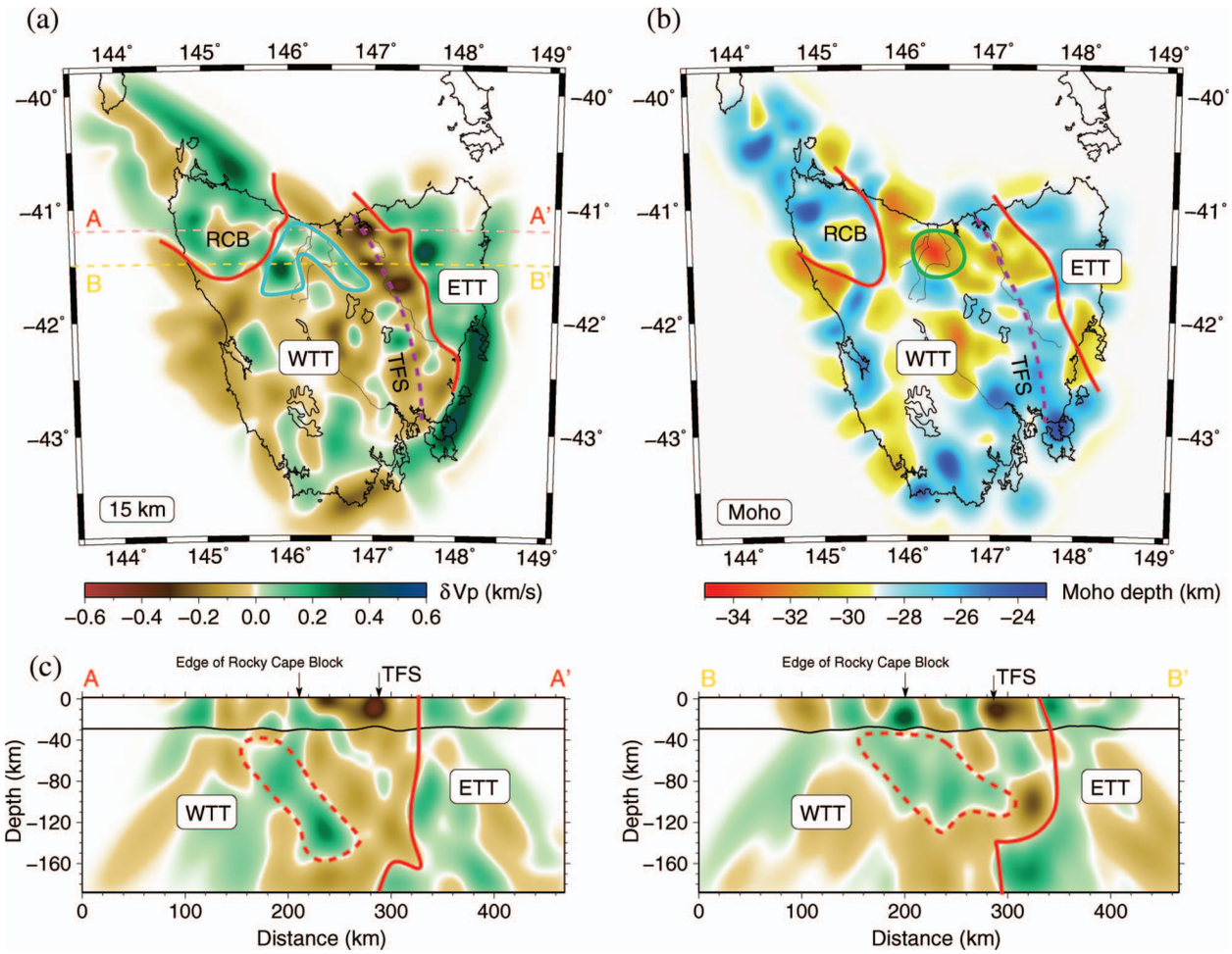

Figure 8 Several different views of the 3D solution model with a number of pertinent features highlighted. (a) 15 km depth slice: the closed curve denotes the region of elevated velocity beneath the Mt Read Volcanics and Forth Metamorphic Complex. (b) Moho depth map: the closed curve denotes the depressed Moho in the vicinity of the Badger Head Block as discussed in the text. (c) Two great circle slices along lines AA′ and BB′ in (a), with a zone of possible remnant subduction indicated by dashed lines. ETT, East Tasmania Terrane; WTT, West Tasmania Terrane; RCB, Rocky Cape Block; TFS, Tamar Fracture System.

to a region of quite thick Cretaceous–Holocene sedimentary rocks (Direen & Leaman 1997); further east, the sediments become thinner, and the underlying crust is intruded by Devonian granites. It is conceivable that the low velocity zone, and hence the marked velocity transition, is at least partly due to the thick sediment layer, and is hence a manifestation of near-surface, unresolved structure. While this is possible, it should be noted that no active source receivers overlie this anomaly, so wide-angle reflection and refraction paths are unlikely to sample the sediment layer at all. In addition, it is unlikely that very shallow structure would smear along the teleseismic ray paths to lower crustal and upper mantle depths.

As well as presenting a new model for the structure and tectonic evolution of the East Tasmania Terrane and its relationship to the West Tasmania Terrane, Reed (2001) also proposed a correlation between Proterozoic rocks in western Tasmania with those underlying the Melbourne Zone in Victoria. Furthermore, he suggested that eastern Tasmania shares an affinity with the Tabberabbera Zone in Victoria, thus implying that the Governor Fault continues southward through Bass Strait and becomes the boundary between the East and West Tasmania Terranes. If this were the case, then our revised location of the paleo-continent–ocean boundary in Tasmania would require less of a dog-leg through Bass Strait (Figure 9; cf. Reed 2001 figure 7) in order to connect up with the Governor Fault.

Rawlinson *et al.* (2001) and Rawlinson & Urvoy (2006) identified a thinner, higher velocity crust beneath the surface expression of the Rocky Cape Block, much as it is here (Figure 8a). One explanation given for this feature was that during the Late Cambrian Tyennan Orogeny, substantial east–west shortening was experienced throughout much of Tasmania, with the exception of the Rocky Cape Block, which behaved as a resistant cratonic block (Turner *et al.* 1998) and therefore was not thickened. Rawlinson & Urvoy (2006) also identified an east-dipping structure in the lithospheric mantle beneath the southeastern edge of the Rocky Cape Block (similar to Figure 8c), which they suggested may be a

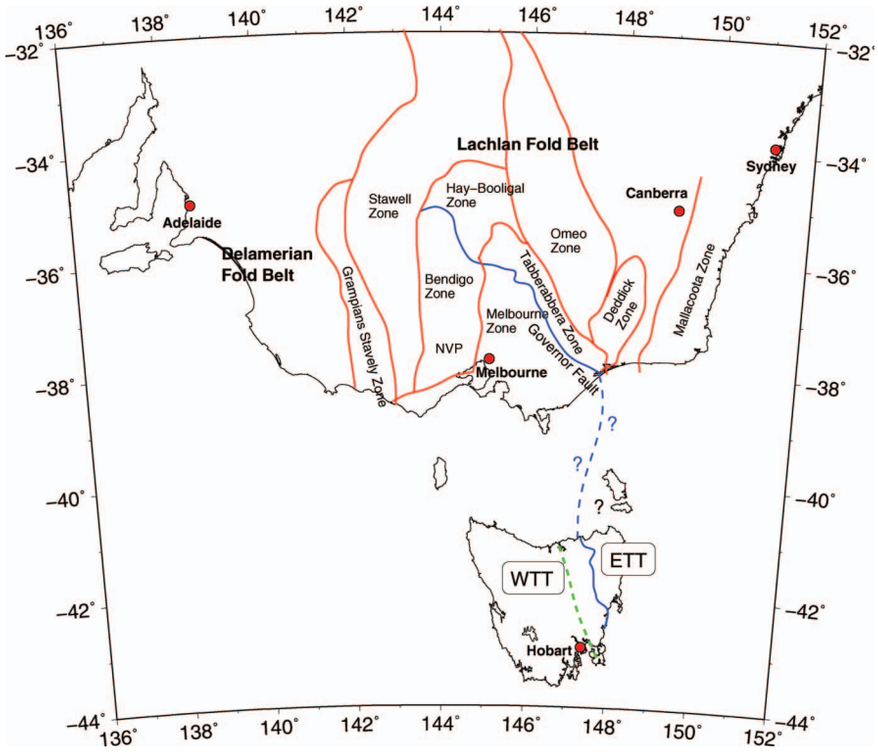

Figure 9 Schematic map showing the possible relationship between Tasmania and mainland Australia. In this scenario, first suggested by Reed (2001), the Paleozoic East Tasmania Terrane (ETT) shares an affinity with the Tabberabbera Zone, while the Proterozoic core of the Western Tasmania Terrane (WTT) is part of a continental fragment extending up beneath the Melbourne Zone (see Cayley *et al.* 2002). The dashed line in Tasmania shows the approximate location of the paleo-continent–ocean boundary according to Reed (2001).

signature of remnant subduction, possibly associated with the Tyennan Orogeny. The presence of Cambrian ophiolites exposed along the eastern margin of the thinner, high velocity crust supports this view. However, although sections AA′ and BB′ in Figure 8c show some evidence of east-dipping mantle structure, remnant subduction is only one of several possible explanations, which also include mantle structure related to the Mt Read Volcanics, and an uneven transition at depth between the Rocky Cape Block and the adjoining terrane to the east. The fact that the east-dipping structure is neither very distinct nor laterally extensive means that plausible alternatives such as these should also be considered.

Two other features of the model that are also present in the results of Rawlinson & Urvoy (2006) are the high velocity crustal anomaly that underlies part of the Cambrian Mt Read Volcanics/Forth Metamorphic Complex (Figure 8a) and a localised Moho depression in almost the same geographic location (Figure 8b). The Mt Read Volcanics is a highly mineralised province that hosts five major gold-rich sulfide deposits (Crawford *et al.* 1992), while the Forth Metamorphic Complex contains schist and amphibolite of Proterozoic origin that were probably partially subducted during a Cambrian arc–continent collision (Meffre *et al.* 2000). The high velocity anomaly may relate to deeper intrusive structures that underpin the volcanic belt, combined with the effects of amphibolite rocks to the north [which tend to have higher velocities (Barberini *et al.* 2007)], or may be due to a lack of constraint on very near-surface wave-speed variations (e.g. a contrast between Tasmania Basin deposits and Cambrian sedimentary and felsic rocks, although these are rather thin, and may not manifest as anomalies at greater depth). The localised Moho depression highlighted in Figure 8b underlies the Port Sorell Block and abuts the Badger Head Block; this region of Tasmania experienced significant shortening (up to 20%) during the Middle Devonian Tabberabberan Orogeny (Elliot and Gray 1992). Reed *et al.* (2002) also observed significant shortening in this region due to the Tyennan Orogeny. It is likely that the Moho depression is related to the crustal thickening that occurred as a result of these events.

The spatial resolution, geographic coverage and vertical penetration of the 3D seismic model of the Tasmanian lithosphere featured in this study is without precedent in Australia; previous seismic-imaging studies either span a much smaller area, or recover much longer wavelength features. In addition, there is further scope for analysis of data from TIGGER and SETA using other complementary seismic techniques, including ambient-noise energy generated by oceanic and atmospheric disturbances, and converted teleseismic phases. In the former case, ambient energy can be used to constrain shallow- to mid-crustal structure, and in the latter case, receiver functions can be extracted and used to image the detailed structure beneath each receiver. This work will be carried out as part of ongoing and future research.

ACKNOWLEDGEMENTS

The use of short period seismic equipment from the ANSIR Major National Research Facility is gratefully acknowledged. N. Direen and G. Green are thanked for their constructive reviews which greatly improved the original manuscript. This research was partly supported by ARC Discovery Project DP0986750.

REFERENCES

AKI K., CHRISTOFFERSSON A. & HUSEBYE E. S. 1977. Determination of the three-dimensional seismic structure of the lithosphere. *Journal of Geophysical Research* **82**, 277–296.

AKI K. & LEE W. H. K. 1976. Determination of the three-dimensional velocity anomalies under a seismic array using first *P* arrival times from local earthquakes 1. A homogeneous initial model. *Journal of Geophysical Research* **81**, 4381–4399.

BARBERINI V., BURLINI L. & ZAPPONE A. 2007. Elastic properties, fabric and seismic anisotropy of amphibolites and their contribution to the lower crust reflectivity. *Tectonophysics* **445**, 227–244.

BENZ H. M., ZANDT G. & OPPENHEIMER D. H. 1992. Lithospheric structure of northern California from teleseismic images of the upper mantle. *Journal of Geophysical Research* **97**, 4791–4807.

BERRY R. F., STEELE D. A. & MEFFRE S. 2008. Proterozoic metamorphism in Tasmania: implications for tectonic reconstructions. *Precambrian Research* **166**, 387–396.

BISHOP T. P., BUBE K. P., CUTLER R. T., LANGAN R. T., LOVE P. L., RESNICK J. R., SHUEY R. T., SPINDLER D. A. & WYLD H. W. 1985. Tomographic determination of velocity and depth in laterally varying media. *Geophysics* **50**, 903–923.

BLEIBINHAUS F. & GEBRANDE H. 2006. Crustal structure of the Eastern Alps along the TRANSALP profile from wide-angle seismic tomography. *Tectonophysics* **414**, 51–69.

BODIN T. & SAMBRIDGE M. 2009. A self-parametrizing partition model approach to tomographic inverse problems. *Inverse Problems* **25**, doi:10.1088/0266-5611/25/5/055009.

BURDICK S., LI C., MARTYNOV V., COX T., EAKINS J., ASTIZ L., VERNON F. L., PAVLIS G. L. & VAN DER HILST R. D. 2008. Upper mantle heterogeneity beneath North America from travel time tomography with global and USArray transportable array data. *Seismological Research Letters* **79**, 384–392.

BURRETT C. F. & FINDLAY R. H. 1984. Cambrian and Ordovician conodonts from the Robertson Bay Group, Antarctica and their tectonic significance. *Nature* **307**, 723–724.

CAYLEY R., TAYLOR D. H., VANDENBERG A. H. M. & MOORE D. H. 2002. Proterozoic–Early Palaeozoic rocks and the Tyennan Orogeny in central Victoria: the Selwyn Block and its tectonic implications. *Australian Journal of Earth Sciences* **49**, 225–254.

CLIFFORD P., GREENHALGH S., HOUSEMAN G. & GRAEBER F. 2008. 3-D seismic tomography of the Adelaide fold belt. *Geophysical Journal International* **172**, 167–186.

COLLINS W. J. 2002. Hot orogens, tectonic switching and creation of continental crust. *Geology* **30**, 535–538.

CRAWFORD A. J. & BERRY R. F. 1992. Tectonic implications of Late Proterozoic–Early Palaeozoic igneous rock associations in western Tasmania. *Tectonophysics* **214**, 37–56.

CRAWFORD A. J., CAYLEY R. A., TAYLOR D. H., MORAND V. J., GRAY C. M., KEMP A. I. S., WOHLT K. E., VANDENBERG A. H. M., MOORE D. H., MAHER S., DIREEN N. G., EDWARDS J., DONAGHY A. G., ANDERSON J. A. & BLACK L. P. 2003b. Neoproterozoic and Cambrian continental rifting, continent–arc collision and post-collisional magmatism. *In*: Birch W. D. ed. *Geology of Victoria*, pp. 73–93. Geological Society of Australia Special Publication **23**.

CRAWFORD A. J., CORBETT K. D. & EVERARD J. L. 1992. Geochemistry of the Cambrian volcanic-hosted massive sulfide-rich Mount Read Volcanics, Tasmania, and some tectonic implications. *Economic Geology* **87**, 597–619.

CRAWFORD A. J., MEFFRE S. & SYMONDS P. A. 2003a. 120 to 0 Ma tectonic evolution of the southwest Pacific and analogous geological evolution of the 600 to 220 Ma Tasman Fold Belt System. *In*: Hillis R. R. & Müller R. D. eds. *Evolution and dynamics of the Australian Plate*, pp. 383–404. Geological Society of Australia Special Publication 22 and Geological Society of America Special Publicaion **372**.

DEBAYLE E. & KENNETT B. L. N. 2000. The Australian continental upper mantle: structure and deformation inferred from surface waves. *Journal of Geophysical Research* **105**, 25423–25450.

DE KOOL M., RAWLINSON N. & SAMBRIDGE M. 2006. A practical grid based method for tracking multiple refraction and reflection phases in 3D heterogeneous media. *Geophysical Journal International* **167**, 253–270.

DIREEN N. G. & CRAWFORD A. J. 2003a. The Tasman Line: where is it, what is it, and is it Australia's Rodinian breakup boundary? *Australian Journal of Earth Sciences* **50**, 491–502.

DIREEN N. G. & CRAWFORD A. J. 2003b. Fossil seaward-dipping reflector sequences preserved in southeastern Australia: a 600 Ma volcanic passive margin in eastern Gondwanaland. *Journal of the Geological Society of London* **160**, 985–990.

DIREEN N. G. & LEAMAN D. E. 1997. Geophysical modelling of structure and tectonostratigraphic history of the Longford Basin, Northern Tasmania. *Exploration Geophysics* **28**, 29–33.

DZIEWONSKI A. M., HAGER B. H. & O'CONNELL R. J. 1977. Large-scale heterogeneities in the lower mantle. *Journal of Geophysical Research* **82**, 239–225.

ELLIOT C. G. & GRAY D. R. 1992. Correlations between Tasmania and the Tasman–Transantarctic orogen: evidence for easterly derivation of Tasmania relative to mainland Australia. *Geology* **20**, 621–624.

FERGUSSON C. L. 2003. Ordovician–Silurian accretion tectonics of the Lachlan Fold Belt, southeastern Australia. *Australian Journal of Earth Sciences* **50**, 475–490.

FISHWICK S., KENNETT B. L. N. & READING A. M. 2005. Contrasts in lithospheric structure within the Australian craton—insights from surface wave tomography. *Earth and Planetary Science Letters* **231**, 163–176.

FOSTER D. A. & GRAY D. R. 2000. Evolution and structure of the Lachlan Fold Belt (Orogen) of eastern Australia. *Annual Review of Earth and Planetary Sciences* **28**, 47–80.

GLEN R. A. 2005. The Tasmanides of eastern Australia. *In*: Vaughan A. P. M., Leat P. T. & Pankhurst R. J. eds. *Terrane processes at the margins of Gondwana*, pp. 23–96. Geological Society of London Special Publication 246.

GORBATOV A. & KENNETT B. L. N. 2003. Joint bulk-sound and shear tomography for Western Pacific subduction zones. *Earth and Planetary Science Letters* **210**, 527–543.

GRAEBER F. M., HOUSEMAN G. A. & GREENHALGH S. A. 2002. Regional teleseismic tomography of the western Lachlan Orogen and Newer Volcanic Province, southeast Australia. *Geophysical Journal International* **149**, 249–266.

GRAND S. P., VAN DER HILST R. D. & WIDIYANTORO S. 1997. Global seismic tomography: a snapshot of convection in the Earth. *GSA Today* **7**, 1–7.

KENNETT B. L. N., ENGDAHL E. R. & BULAND R. 1995. Constraints on seismic velocities in the earth from travel times. *Geophysical Journal International* **122**, 108–124.

KENNETT B. L. N., SAMBRIDGE M. S. & WILLIAMSON P. R. 1988. Subspace methods for large scale inverse problems involving multiple parameter classes. *Geophysical Journal* **94**, 237–247.

LEAMAN D. E. 1994. The Tamar Fracture System in Tasmania: does it exist? *Australian Journal of Earth Sciences* **41**, 73–74.

LEAMAN D. E., BAILLIE P. W. & POWELL C. MCA. 1994. Precambrian Tasmania: a thin-skinned devil. *Exploration Geophysics* **25**, 19–23.

LI Z. X., BAILLIE P. W. & POWELL C. MCA. 1997. Relationship between northwestern Tasmania and East Gondwanaland in the Late Cambrian/Early Ordovician: paleomagnetic evidence. *Tectonics* **16**, 161–171.

MCMECHAN G. A. 1987. Cross-hole tomography for strongly variable media with applications to scale model data. *Bulletin of the Seismological Society of America* **77**, 1945–1960.

MEFFRE S., BERRY R. F. & HALL M. 2000. Cambrian metamorphic complexes in Tasmania: tectonic implications. *Australian Journal of Earth Sciences* **47**, 971–985.

MEFFRE S., DIREEN N. G., CRAWFORD A. J. & KAMENETSKY V. S. 2004. Mafic volcanic rocks on King Island, Tasmania: evidence for 579 Ma break-up in east Gondwana. *Precambrian Research* **135**, 177–191.

MOONEY W. D., LASKE G. & MASTERS T. G. 1998. CRUST 5.1: a global crustal model at $5^\circ \times 5^\circ$. *Journal of Geophysical Research* **103**, 727–747.

POWELL C. MCA. & BAILLIE P. W. 1992. Tectonic affinity of the Mathinna Group in the Lachlan Fold Belt. *Tectonophysics* **214**, 193–209.

POWELL C. MCA., LI Z. X., THRUPP G. A. & SCHMIDT P. W. 1990. Australian Palaeozoic palaeomagnetism and tectonics—I. Tectonostratigraphic terrane constraints from the Tasman Fold Belt. *Journal of Structural Geology* **12**, 553–565.

PRIESTLEY K., MCKENZIE D., DEBAYLE E. & PILIDOU S. 2008. Upper-mantle velocity structure beneath the Siberian platform. *Geophysical Journal International* **118**, 369–378.

RAWLINSON N., HOUSEMAN G. A., COLLINS C. D. N. & DRUMMOND B. J. 2001. New evidence of Tasmania's tectonic history from a novel seismic experiment. *Geophysical Research Letters* **28**, 3337–3340.

RAWLINSON N. & KENNETT B. L. N. 2004. Rapid estimation of relative and absolute delay times across a network by adaptive stacking. *Geophysical Journal International* **157**, 332–340.

RAWLINSON N., KENNETT B. L. N. & HEINTZ M. 2006b. Insights into the structure of the upper mantle beneath the Murray Basin from 3D teleseismic tomography. *Australian Journal of Earth Sciences* **53**, 595–604.

RAWLINSON N., READING A. M. & KENNETT B. L. N. 2006a. Lithospheric structure of Tasmania from a novel form of teleseismic tomography. *Journal of Geophysical Research* **111**, doi:10.1029/2005JB003803.

RAWLINSON N. & SAMBRIDGE M. 2003. Seismic traveltime tomography of the crust and lithosphere. *Advances in Geophysics* **46**, 81–198.

RAWLINSON N. & URVOY M. 2006. Simultaneous inversion of active and passive source datasets for 3-D seismic structure with application to Tasmania. *Geophysical Research Letters* **33**, doi:10.1029/2006GL028105.

REED A. R. 2001. Pre-Tabberabberan deformation in eastern Tasmania: a southern extension of the Benambran Orogeny. *Australian Journal of Earth Sciences* **48**, 785–796.

REED A. R., CALVER C. & BOTTRILL R. S. 2002. Palaeozoic suturing of eastern and western Tasmania in the west Tamar region: implications for the tectonic evolution of southeast Australia. *Australian Journal of Earth Sciences* **49**, 809–830.

SETHIAN J. A. & POPOVICI A. M. 1999. 3-D traveltime computation using the fast marching method. *Geophysics* **64**, 516–523.

SIMONS F., ZIELHUIS A. & VAN DER HILST R. 1999. The deep structure of the Australian continent from surface wave tomography. *Lithos* **48**, 17–43.

SPAGGIARI C. V., GRAY D. R. & FOSTER D. A. 2004. Lachlan Orogen subduction–accretion systematics revisited. *Australian Journal of Earth Sciences* **51**, 549–553.

SPAGGIARI C. V., GRAY D. R., FOSTER D. A. & MCKNIGHT S. 2003. Evolution of the boundary between the western and central Lachlan Orogen: implications for Tasmanide tectonics. *Australian Journal of Earth Sciences* **50**, 725–749.

STECK L. K., THURBER C. H., FEHLER M., LUTTER W. J., ROBERTS P. M., BALDRIDGE W. S., STAFFORD D. G. & SESSIONS R. 1998. Crust and upper mantle P wave structure beneath Valles caldera, New Mexico: results from the Jemez teleseismic tomography experiment. *Journal of Geophysical Research* **103**, 24301–24320.

SUTHERLAND F. L. 2003. 'Boomerang' migratory intraplate Cenozoic volcanism, eastern Australian rift margins and the Indian–Pacific mantle boundary. *In*: Hillis R. R. & Müller R. D. eds. *Evolution and dynamics of the Australian Plate*, pp. 203–221. Geological Society of Australia Special Publication **22** and Geological Society of America Special Publication **372**.

TALENT J. A. & BANKS M. R. & 1967. Devonian of Victoria and Tasmania. *In*: Oswald D. H. ed. *International Symposium on the Devonian System, Calgary*, vol. 2, pp. 147–163. Alberta Society of Petroleum Geologists, Calgary.

TURNER N. J., BLACK L. P. & KAMPERMAN M. 1998. Dating of Neoproterozoic and Cambrian orogenies in Tasmania. *Australian Journal of Earth Sciences* **45**, 789–806.

VANDENBERG A. H. M. 1999. Timing of orogenic events in the Lachlan Orogen. *Australian Journal of Earth Sciences* **46**, 691–701.

VEEVERS J. J. & EITTREIM S. L. 1988. Reconstruction of Antarctica and Australia at breakup (95 ± 5 Ma) and before rifting (160 Ma). *Australian Journal of Earth Sciences* **35**, 355–362.

WALCK M. C. 1988. Three-dimensional V_p/V_s variations for the Coso region, California. *Journal of Geophysical Research* **93**, 2047–2052.

WILLIAMS E. 1989. Summary and synthesis. *In*: Burrett C. F. & Martin E. L. eds. *Geology and mineral resources of Tasmania*, pp. 468–499. Geological Society of Australia Special Publication **15**.

WILLIAMSON P. R. 1990. Tomographic inversion in reflection seismology. *Geophysical Journal International* **100**, 255–274.

WILLMAN C. E., VANDENBERG A. H. M. & MORAND V. J. 2002. Evolution of the southeastern Lachlan Fold Belt in Victoria. *Australian Journal of Earth Sciences* **49**, 271–289.

ZELT C. A. & WHITE D. J. 1995. Crustal structure and tectonics of the southeastern Canadian Cordillera. *Journal of Geophysical Research* **100**, 24255–24273.

ZIELHUIS A. & VAN DER HILST R. D. 1996. Mantle structure beneath the eastern Australia region from partitioned waveform inversion. *Geophysical Journal International* **127**, 1–16.

Received 27 September 2009; accepted 5 March 2010